Phase Diagrams of Non-Ionic Microemulsions Containing Reducing Agents and Metal Salts as Bases for the Synthesis of Bimetallic Nanoparticles

Miguel Magno[1], Daniel G. Angelescu[1,2*], Cosima Stubenrauch[1]

[1] *University College Dublin, School of Chemical and Bioprocess Engineering, Centre for Synthesis and Chemical Biology (CSCB), SFI-Strategic Research Cluster in Solar Energy Conversion, University College Dublin, Belfield, Dublin 4, Ireland*

[2] *Institute of Physical Chemistry, "I.G. Murgulescu" Romanian Academy, Splaiul Independentei 202, 060021 Bucharest, Romania*

*corresponding author; e-mail: daniel.angelescu@ucd.ie

Abstract

Phase diagrams of microemulsions containing metal salt(s) and reducing agent, respectively, were studied in detail. The microemulsions were based on non-ionic surfactants, namely pure tetraethyleneglycol monododecylether, $C_{12}E_4$, and technical grade Brij30. We studied the influence of the metal salts H_2PtCl_6, $Pb(NO_3)_2$, $Bi(NO_3)_3$, H_2PtCl_6 + $Pb(NO_3)_2$ (1:1 mixture), and H_2PtCl_6 + $Bi(NO_3)_3$ (1:1 mixture) as well as of the reducing agent $NaBH_4$ on the location of the phase boundaries. The focus was on the water emulsification failure boundary (*wefb*) where the aqueous phase forms spherical droplets. The temperature shifts of the *wefb*, which were caused by the presence of the salt(s), are directly related with the shift of the clouding points of the corresponding oil-free systems. The location of the *wefb* is affected in a complex manner by the pH (the lower the pH the higher the temperature at which the *wefb* occurred), the ionic strength and by specific salting-in or salting-out effects of the electrolyte ions. The desired overlap of the *wefb* of the microemulsions containing the metal salt(s) and the reducing agent, respectively, could be achieved by adding NaOH to the $C_{12}E_4$-based microemulsions and by titrating 1-octanol to the Brij30-based microemulsions, respectively.

Keywords: water emulsification failure boundary, funnel phase diagrams, non-ionic surfactants, w/o-microemulsions as nanoreactors, monometallic and bimetallic nanoparticles

1. Introduction

The self-assembly of surfactants into structures with well-defined size and shape has been exploited over the past two decades for the synthesis of nanoscale inorganic materials. One important area of surfactant-supported synthesis of nanomaterials is the microemulsion-based synthesis of metallic nanoparticles. Various materials, mainly metals and metal oxides, have been prepared following this procedure. Microemulsions are defined as isotropic, macroscopically homogeneous and thermodynamically stable mixtures containing a polar phase such as water, a non-polar phase such as oil, and a surfactant that forms an interfacial film separating the polar and non-polar domains. Depending on the composition and temperature, the microstructure of microemulsions ranges from oil droplets dispersed in the continuous aqueous phase, *i.e.* oil-in-water microemulsions, over a bicontinuous structure, to droplets of the aqueous phase dispersed in the continuous oil phase, *i.e.* water-in-oil microemulsions. For the synthesis of metallic nanoparticles the metal source, *e.g.* a metal salt, is solubilized in the aqueous phase of a water-in-oil microemulsion, whereas the reducing agent, such as hydrazine or sodium borohydride, is added either as a solid compound[1-3], solubilised in a second water-in-oil microemulsion[4-9] or in a solvent.[10] Excellent reviews of the synthesis of inorganic nanoparticles via microemulsions are refs. [11], [12] and [13]. Once both metal salt and reducing agent are solubilised in water-in-oil microemulsions, an exchange between the aqueous phases of the two microemulsions occurs via a fusion-fission process,[11] and the metal salt and reducing agent will eventually be distributed evenly throughout the aqueous phase. At the same time, the metal reduction will take place in the aqueous phase resulting in monodisperse inorganic nanoparticles. Although the water droplet size seems to have an effect on the size of the particles,[7][8, 9, 14-16] the nucleation and growth of the particles is not understood yet. In some systems the resulting particles were

found to be of the same size, while in other systems they were much larger than the water droplets.[17, 18]

The presence of more than one metal in the metallic nanoparticles is of particular interest since the physical and chemical interactions between different atoms can lead to new properties. For example, it turned out that combining a transition metal with platinum enhances the catalytic activities for reactions such as oxygen reduction in fuel cells and direct oxidation of methanol as compared to the pure Pt catalyst.[19, 20] A number of techniques have been used for producing bimetallic nanoparticles for fuel cells which include single spontaneous deposition,[21] furnace melting and thermal annealing,[22-24] sputtering,[25] reducing of metal salt in aqueous solution[26] as well as the solvochemical reduction method[27-29] and the polyol process.[30] The microemulsion method was also pursued to prepare Pt-metal catalysts for oxygen reduction in fuel cells.[1, 16, 31-34] It is believed that the synthesis of the particles at low temperatures as well as their narrow size distribution leads to better catalytic activity.[31, 35] However, the synthesis of Pt-metal intermetallic particles via the microemulsion route was reported only for metals with similar reduction potential, such as Pt:Ag,[36] Pt:Au[37] and Pt:Pd,[38][39] while the synthesis using metals with largely different reduction potentials has not yet been achieved.

To the best of our knowledge, there are only four studies dealing with the phase diagram and stability of microemulsions containing metal salt and reducing agent.[18, 33, 40, 41] Stubenrauch et al [18, 41] studied in detail the phase behaviour of the system H_2O/metal salt(s) - *n*-decane – SDS/1-butanol. The focus was on the determination of the water emulsification failure boundary (*wefb*) along which the aqueous phase forms spherical droplets over a large concentration range.[42-44] It was shown that the ionic strength and the hard acid and hard base properties of the charged ions had a pronounced effect on the location of the *wefb* and, consequently, these parameters have to be carefully tuned in order to obtain the desired spherical droplets of same size containing the metal salt and reducing agent,

respectively. It was found that nanoparticles of Pt, Bi and Pb synthesized with the system H_2O/metal salt(s) - *n*-decane – sodium dioctyl sulfosuccinate (AOT)/SDS/1-butanol were different in size although the size of the precursor microemulsion droplets was the same. The resulting Pt nanoparticles were much smaller than the Bi and Pb nanoparticles. Malheiro et al.[33] studied the phase behavior of the system H_2O/metal salts - *n*-heptane - AOT/*n*-butanol and used it for the synthesis of Pt:Fe bimetallic nanoparticles. It turned out that the addition of *n*-butanol as co-surfactant influenced the composition of the bimetallic particles, whereas the average crystallite diameter and the mean particle size remained unchanged. These results indicate that not only the water droplet size in the precursor microemulsions but also the interplay between the material exchange during the fusion-fission process, the reducing rate of the metal salt, and the mutual self-diffusion of the water droplets determine the size of the as-synthesized nanoparticles. Recent simulations support these experimental findings.[45]

Since the self-assembly of non-ionic surfactants is less sensitive to the addition of electrolytes compared to that of ionic surfactants, the structure of non-ionic surfactant-based microemulsions should be less affected by the addition of metal salts and reducing agent. Several syntheses of Pt and Pt:Metal particles via microemulsions using non-ionic surfactant have been reported in the past few years.[8, 32, 34, 38, 46] It was found that the platinum ions have little effect on the water droplet size and that the reaction rate of platinum particle formation was considerable lower in microemulsions based on non-ionic alkyl polyethyleneoxide surfactants compared to microemulsions based on AOT.[8] The size of the synthesized particles was lower than 7 nm,[8, 32, 34] the particles had a narrow size distribution,[32] and the bimetallic particles were found to be larger than the pure counterparts.[38] Alloyed[32, 46] and core-shell particles[38] were reported and it was shown that the electrocatalytic properties can be enhanced by increasing the amount of metal in the platinum-metal alloys.[34, 46]

In the present study the influence of the metal salt and the reducing agent on the phase behavior of microemulsions stabilized by either pure or technical grade alkyl polyethyleneoxide surfactants is studied systematically. As the final goal is to synthesize monometallic Pt, Pb, and Bi as well as bimetallic Pt:Pb and Pt:Bi particles of controlled size, the aqueous phase of the microemulsions contained the metal salts H_2PtCl_6, $Pb(NO_3)_2$, and $Bi(NO_3)_3$, 1:1 mixtures of H_2PtCl_6 + $Pb(NO_3)_2$ and H_2PtCl_6 + $Bi(NO_3)_3$, and the reducing agent $NaBH_4$, respectively. To characterize the resulting systems the approach presented in ref. [41] is followed, i.e. the *wefb* has been determined carefully for all systems. The demand of determining this boundary for precursor microemulsions is given by the fact that at it the water droplets are spherical and their size is controlled by the water content. We will also demonstrate how the *wefb* can be tuned such that the *wefb* of the microemulsion containing the metal salt and the reducing agent, respectively, overlap, which is the prerequisite for equal water droplet sizes in both microemulsions .

2. Materials and Methods

2.1. Materials

n-octane (99.5%) was purchased from Fluka, while 1-octanol (99%), NaCl (99.99%), HCl (37 % v/v) and NaOH (99%) were obtained from Sigma Aldrich. The pure non-ionic surfactant tetraethyleneglycol monododecylether (98%), abbreviated as $C_{12}E_4$, was supplied by Fluka and the technical grade one which contains an average of four ethylene oxide groups, referred to as Brij30, was purchased from Sigma Aldrich. The metal salts hexachloroplatinic acid ($H_2PtCl_6 \cdot 6H_2O$, 99.9%), lead (II) nitrate ($Pb(NO_3)_2$, 99.999%), bismuth (III) nitrate pentahydrate ($Bi(NO_3)_3 \cdot 5H_2O$, 99.999%) and the reducing agent sodium borohydride

($NaBH_4$, 99%) were also supplied by Sigma Aldrich. All chemicals were used without further purification. The water used was treated with a Millipore-Q water purification system.

2.2. Sample preparation and determination of phase diagrams

The samples were made by diluting the stock solution containing the non-polar solvent B (*n*-octane), surfactant C and co-surfactant D (1-octanol) with the aqueous phase (A) (water or solute-containing aqueous solution). Appropriate amounts of *n*-octane and surfactant and/or co-surfactant were weighted into test tubes sealed thereafter with stoppers. After homogenization under stirring, the aqueous phase was added. The sample composition is given by the following parameters:

- the mass fraction of surfactant, $C_{12}E_4$ or Brij30 (C), and co-surfactant, 1-octanol (D), in the oil phase

$$\gamma_b = \frac{m_C + m_D}{m_B + m_C + m_D}, \quad (1)$$

- the mass fraction of co-surfactant, 1-octanol (D), in the mixture of 1-octanol and Brij30

$$\delta = \frac{m_D}{m_C + m_D}, \quad (2)$$

- the overall mass fraction of the aqueous phase (A)

$$w_A = \frac{m_A}{\sum_i m_i}, \quad (3)$$

- the mass fraction (or molar concentration alternatively) of the dissolved inorganic solute (metal salt, electrolyte or reducing agent) in the aqueous phase (A)

$$\varepsilon = \frac{m_{solute}}{m_{solute} + m_A} \quad (4)$$

The phase boundaries were determined starting from the two-phase region (where the sample had either a pronounced turbidity or a milky appearance) by increasing or decreasing the temperature (under continuous stirring) followed by sample equilibration at the desired temperature. The macroscopic phase separation between the microemulsion and the excess phases was slow, especially next to the phase boundaries. The sample turbidity was determined by visual inspection and verified by turbidity measurements at $\lambda = 450$ nm with an Agilent 8453 spectrophotometer. A good agreement of the two methods was found unless the water content w_A was less than 0.06. The accuracy in determining the phase boundaries of the pure and the technical grade surfactant based microemulsions was 0.2 °C and 0.8 °C, respectively.

It should be noted that the droplet size of the microemulsion was difficult to assess from the turbidity measurements due to the much lower turbidity of the oil-rich microemulsion as compared to corresponding water-rich microemulsion.[47]

Finally, several remarks should be made. Firstly, a very slow reduction of Bi^{3+} and Pb^{2+} (occurring on a time-scale of about ten hours) caused by the alcohol (1-octanol)[48, 49] was observed only at low water content ($w_A < 0.8$) when either the oil-in-water microemulsion coexisted with an oil phase for several hours or at temperatures higher than 50 °C. Secondly, due to the formation of $NaBO_2$ in aqueous solution, fresh $NaBH_4$ was prepared for each sample before starting the measurements. Thirdly, to prevent the formation of water-insoluble BiO^+ (bismuthyl ion), the bismuth nitrate solution was made acidic by adding nitric acid. Hence 0.04 M $Bi(NO_3)_3$ was solubilized in 0.32 M HNO_3 whereas for the mixture of 0.011 M H_2PtCl_6 and 0.011 M $Bi(NO_3)_3$ a 2 M HNO_3 solution was prepared. Fourthly, the oxidation sensitive lead and bismuth containing samples were neither degassed with inert gas flow nor handled under inert gas atmosphere at this stage since we were only interested in the phase behaviour of the precursor systems which are not sensitive to oxidation. For the synthesis of the particles the solutions will be degassed and handled under inert gas.

3. Results and Discussions

Our approach towards the synthesis of metallic nanoparticles of controlled size is to mix a water-in-oil microemulsion that contains one or more metal salts with one that contains the reducing agent. To study the correlation between water droplet and particle size, the water droplets of the two precursor microemulsions should be the same. To achieve this demand we decide to measure the *wefb* of the precursor microemulsions as it is at this phase boundary where the water droplets are spherical and where the size of the droplets can be controlled by the water content.[50] The diameter *d* of the spherical droplets at the *wefb* can be calculated according to

$$d = 6\delta \frac{\phi_{disp}}{\phi_{C,i} + \phi_{D,i}} \approx 6nm \frac{w_A + \gamma}{\gamma} \qquad (5)$$

where $\delta \approx$ 1 nm is the thickness of the amphiphilic interfacial film, ϕ_{disp} is the volume fraction of the dispersed phase, and $\phi_{C,i}$ and $\phi_{D,i}$ are the volume fractions of the surfactant and co-surfactant forming the interface.[51] This equation provided us a simple method to estimate the size of the droplets at any w_A value. As for example, the estimated diameter of the water droplets at *wefb* for the system **H_2O/solute – *n*-octane – $C_{12}E_4$** at γ_b = 0.06 and w_A = 0.06 was 18 nm. Complementary determination of the droplet size by light scattering technique leading to more insights of the relationship between the water droplet diameter and the as-synthesized particle size is under progress.

In section 3.1 we will first present the phase diagram as two-dimensional $T(w_A)$-cut of microemulsions stabilized by the pure non-ionic surfactant dodecyl tetraethyleneoxide, $C_{12}E_4$. In section 3.2 we will replace $C_{12}E_4$ by the technical grade surfactant Brij30, discuss the results and investigate the role of the co-surfactant 1-octanol in stabilizing Brij30-based

microemulsions at room temperature. For both systems the water emulsification failure boundaries (*wefb*) of microemulsions containing pure water, one or two of the three metal salts H_2PtCl_6, $Bi(NO_3)_3$, and $Pb(NO_3)_2$, and the reducing agent $NaBH_4$, respectively, will be presented and compared. Finally a route how to obtain *wefb*s at the same temperature for different microemulsions will be described.

3.1. The Systems H_2O/solute – *n*-octane – $C_{12}E_4$

3.1.1. Phase Diagrams of H_2O/solute – *n*-octane – $C_{12}E_4$

Starting point was the ternary base system **H_2O – *n*-octane – $C_{12}E_4$** to which we added either a metal salt (H_2PtCl_6, $Pb(NO_3)_3$, $Bi(NO_3)_3$) or the reducing agent ($NaBH_4$). We measured the phase boundaries as a function of the content of the aqueous phase w_A at a fixed surfactant mass fraction in the oil phase of $\gamma_b = 0.06$. The resulting $T(w_A)$-sections, the so-called funnel diagrams, are displayed in Figure 1 and 2 and the compositions of the aqueous phases are given in Table 1. For the sake of comparison the phase diagram of the ternary base system is shown in both figures.

Figure 1

Figure 2

Table 1

The main feature of the phase diagram of the reference system is the one-phase, funnel-shaped microemulsion region, which closes at the endpoint characterized by $w_A \sim 0.16$ and T_u

~ 14 °C. A water content w_A larger than 0.16 cannot be solubilised at γ_b = 0.06 and thus a phase separation occurs. For w_A < 0.16 and low temperatures, oil coexists with an oil-in-water microemulsion (region $\underline{2}$), whereas at elevated temperatures water coexists with a water-in-oil microemulsion (region $\bar{2}$). If one looks at the phase boundaries more closely, it can be seen that the $\underline{2}\rightarrow 1$ phase boundary starts at low temperatures for very low water content (w_A < 0.05, not seen in Figure 1) and increases steeply with increasing water content, reaching a maximum at w_A ~ 0.11. After that it steadily decreases until the critical endpoint is reached. On the other hand, the water emulsification failure boundary, ($\bar{2}\rightarrow 1$), referred to as *wefb*, begins at elevated temperatures and lowers monotonously with increasing water content until the phase inversion is reached. Hence, it can be argued that the temperature range in which both water and oil are solubilized in one phase decreases with increasing water content. Keeping w_A constant one can tune the amount of oil (or water) that can be solubilised in water (or oil) by changing the temperature.

Looking at Figure 1a one sees that addition of 0.04 M (ε = 0.0164) H_2PtCl_6 to the aqueous phase (i) does not change the surfactant efficiency, *i.e.* the highest water content that can be solubilised is still w_A ~ 0.16 and (ii) shifts the phase boundaries to slightly higher temperatures. The surfactant efficiency was also not significantly affected by the addition of 0.04 M (ε = 0.0132) $Pb(NO_3)_2$ (Figure 1b) and 0.04 M (ε = 0.0194) $Bi(NO_3)_3$ (Figure 1c), respectively, while both phase boundaries shift towards higher temperatures as was the case for the first salt. The temperature raise is modest and similar for H_2PtCl_6 and $Pb(NO_3)_2$, while it is significant for the system **H_2O/$Bi(NO_3)_3$ – *n*-octane – $C_{12}E_4$,** namely ~ 4 °C compared to the base system. The mismatch of the phase boundaries is quantified in Table 1, where the temperatures for the sequence transition $\underline{2}\rightarrow 1\rightarrow\bar{2}$ at w_A= 0.06 are given. One can also see in Table 1 how the ionic strength increases once the metal salt is added and that the pH is acidic for the H_2PtCl_6 and the $Bi(NO_3)_3$ system. In the latter case the low pH is caused

by the high content of HNO_3 that had to be added to solubilise the Bi-salt. The reason for the temperature shifts of the phase boundaries will be discussed in section 3.1.2.

Figure 2 compares the phase diagram of the system containing 0.16 M (ε = 0.006) $NaBH_4$ with that of the reference system. As can clearly be seen, the surfactant efficiency again is not affected by the addition of $NaBH_4$, while the phase transitions $\underline{2} \rightarrow 1 \rightarrow \bar{2}$ occur at lower temperatures. This trend is even more pronounced if 0.16 M NaOH are added to the solution, which may be necessary to avoid the formation of sodium metaborate, i.e. to stabilise $NaBH_4$ in aqueous solutions. Thus an increase of the pH leads to a downward shift of the phase boundaries, while a decrease of the pH shifts the phase boundaries towards higher temperatures. A more detailed discussion of this observation will be given in the following.

3.1.2. Tuning the *wefb* of H_2O/solute – *n*-octane – $C_{12}E_4$

In order to better understand the effect of the metal salts and the reducing agent on the funnel phase diagram of the oil-rich region of the system H_2O/**solute – *n*-octane – $C_{12}E_4$**, we studied the effect of salt and of the pH on the phase boundaries in more detail. For this purpose we first exchanged water with 0.16 M of an 1:1 electrolyte solution (NaCl) and measured the respective $T(w_A)$-section at γ_b = 0.06 (see Figure S1 in Supporting Material). Secondly, the ionic strength was kept constant and the pH was varied by addition of 0.16 M HCl, NaCl, and NaOH, respectively. The phase boundaries were determined at γ_b = 0.06 and w_A = 0.08 and plotted versus the pH. The result is seen in Figure 3.

Figure 3

Comparing the location of the phase boundaries of the salt-free and the salt-containing system (Figure S1 in Supporting Material) one sees that the increase of the ionic strength led to a shift

towards lower temperatures. Regarding the pH effect it was found that the characteristic temperatures of both the *wefb* and the $\underline{2}\rightarrow 1$ boundary decreased continuously with increasing pH, the shift being ~2 °C for 6 pH units (Figure 3). These effects may be correlated with the dependence of the cloud point of non-ionic surfactant systems on the inorganic salt content and on the presence of strong acids or bases. It was demonstrated that lyotropic salts like NaCl lead to a decrease of the cloud point.[52, 53] Moreover acids were found to increase while bases were found to decrease the clouding point of non-ionic alkyl polyethyleneoxide surfactants and ethoxylated block-copolymers in aqueous solutions.[54-56] This implies that the mechanism involved in both cases - adding electrolyte and changing pH - has to be similar. Consequently adding solute to the aqueous phase of the microemulsion may be viewed as altering the hydration of the EO groups and can be understood in terms of salting-in (increase of the clouding point) and salting-out (decrease of the clouding point) effects of the cations and anions, respectively.

The location of the *wefb* is also affected by the nature of the added electrolyte, i.e. of the added metal salt. It is known that simple anions increase or decrease the cloud point according to their position in the Hofmeister series,[55, 57] while cations act less effectively and in an indiscriminate manner. The specific effect of electrolytes would explain why the funnel diagrams of the microemulsions containing 0.04 M $Pb(NO_3)_2$ and 0.04 M H_2PtCl_6 (see Figures 1a and b) are similar although the ionic strength and the pH were different (see Table 1). In the case of $Pb(NO_3)_2$ the shift of the phase boundaries to higher temperatures is due to the salting-in effect of NO_3^{-2}.[58] Regarding the effect of H_2PtCl_6 the shift is in agreement with Figure 3, where it was shown that a decrease of the pH by ~6 units leads to an increase of the phase boundaries by roughly 2°C, which is indeed the case for the platinum salt. On the other hand the large highly polarisable $PtCl_6^{2-}$ anions are expected to have a salting-out effect which is obviously compensated for by the pH decrease. The salting-in effect of NO_3^- in combination with the pH decrease also explain the large shift of the funnel diagram observed

for the system **$H_2O/Bi(NO_3)_3/HNO_3$ – *n*-octane – $C_{12}E_4$** (Figure 1c). Comparing the effect of the metal salts with that of the reducing agent (Figure 2) one sees that the latter has an opposite effect on the phase boundaries. The significant shift of the boundaries towards lower temperatures shows that both BH_4^- and OH^- have a strong salting-out effect. Note that the shift is in line with Figure 3 as the pH of both solutions ($NaBH_4$ and $NaBH_4$ + NaOH) is high. In conclusion one can say that the shift of the phase boundaries depends in a complex way on the ionic strength, the pH, and specific ion effects. At this stage and age predicting the effect of metal salts and reducing agents on the phase boundaries is impossible which, in turn, makes an experimental determination of phase boundaries indispensable. [58][59]

Let us come back to the question how to tune the *wefb* such that the *wefb* of the microemulsion containing the metal salt and that of the microemulsion containing the reducing agent are the same (or at least similar). We saw in Figure 1 and 2 that the metal salts and the reducing agents have opposite effects on the phase boundaries. In other words, the phase transition temperatures of the metal salt-containing microemulsions have to be reduced or those of the $NaBH_4$-containing system have to be increased. We also learnt that the phase boundaries shift towards lower temperatures with increasing pH. Thus the approach to match the *wefb* of the two relevant microemulsions was to increase the pH of the metal salt containing systems and thus to decrease the respective phase boundaries (decreasing the pH of the $NaBH_4$-containing system was no option as $NaBH_4$ is rapidly reduced to $NaBO_2$ in neutral or acid solution). That this approach leads indeed to the desired shift of the phase boundaries is demonstrated in Figure 4.

Figure 4

As can be seen in Figure 4 the *wefb* of the two precursor systems nearly overlap, which means that the size and shape of the water pools is roughly the same at a fixed water content and

temperature. Thus a change of the pH indeed shifts the phase boundaries in the desired way and leads to a very good overlap for the microemulsions containing the Pt-salt and $NaBH_4$, respectively. Unfortunately, this approach did work neither for the Pb- nor for the Bi-salt because the addition of NaOH led to the formation of PbO and to the insolubility of Bi^{3+} ion, respectively.

To conclude this chapter we like to emphasize again that for the controlled synthesis of metallic particles it is desirable that the two microemulsions containing the metal salt and the reducing agent, respectively, have the same oil, water and surfactant content as well as the same size of the water droplets. As argued above, the latter implies an overlap of the *wefb* of the two microemulsions which does not occur since the metal salts have an opposite effect on the location of the *wefb* as compared with the reducing agent. In other words, water droplets of *same* size are obtained at *different* temperatures. One possible way out of this dilemma is the addition of NaOH to the metal salt solutions. However, this turned out to be possible for the H_2PtCl_6 only. Nonetheless, this drawback can be overcome by (i) partial replacement of the oil in one of the two microemulsions by another oil or (ii) addition of a co-surfactant, e.g. an alcohol. We followed the second route which will be shown in section 3.2.

3.2. The Systems H_2O/solute – *n*-octane – Brij30/1-octanol

3.2.1. Phase Diagrams of H_2O/solute – *n*-octane – Brij30/1-octanol

What is addressed in this section is the effect the exchange of the pure non-ionic surfactant $C_{12}E_4$ by the technical grade surfactant Brij30 (non-ionic surfactant with an average of four ethylene oxide units as head group) has on the phase behavior. Figure 5 shows the respective $T(w_A)$-sections of the two microemulsions at $\gamma_b = 0.06$.

Figure 5

Strikingly, though the overall molecular structure of Brij30 is the same as that of $C_{12}E_4$, there are dramatic changes once the technical grade surfactant is used to stabilise the microemulsion. Firstly, the surfactant efficiency decreases, which is reflected in the shift of the critical endpoint towards lower w_A-values. Secondly, the one phase region becomes narrower. Thirdly, the temperature range of the one-phase region increases by ~50 °C. These trends can be understood by taking into account the wide distribution of ethylene oxide units in the surfactant head group of Brij30. The more hydrophilic surfactants, i.e. $C_{12}E_j$ with j larger than 4, are preferentially adsorbed at the water-oil interface, while the more hydrophobic surfactants, i.e. $C_{12}E_j$ with j smaller than 4, are solubilised in the oil phase, thus rendering the interface much more hydrophilic than it would be in the case of pure $C_{12}E_4$. To obtain a funnel diagram with an appearance similar to that of the system **H_2O – *n*-octane – $C_{12}E_4$** and a considerable drop of the temperature range of the one-phase region 1-octanol was added. The result is also shown in Figure 5. One can see that by adding 1-octanol to Brij30 γ_b increases from 0.06 to 0.114, the one-phase channel extends to larger w_A, and the funnel diagram is found at lower temperatures. Note that the partitioning of the alcohol between the oil phase (acting as co-solvent) and the interface (acting as co-surfactant) was not addressed in this study.

Following the same route as for the system **H_2O/solute – *n*-octane – $C_{12}E_4$**, we investigated the effect of the various metal salts (H_2PtCl_6, $Pb(NO_3)_2$, $Bi(NO_3)_3$) and the reducing agent ($NaBH_4$) on the phase behaviour of the systems **H_2O/solute – *n*-octane – Brij30/1-octanol**. Again, we measured the funnel diagrams at constant γ_b- and δ-value. Results for microemulsions containing H_2PtCl_6, $Pb(NO_3)_2$ and $NaBH_4$ are given in Figure 6.

Figure 6

As is seen in Figure 6, the presence of 0.16 mM $NaBH_4$ leads to a pronounced shift of the *wefb* towards lower temperatures, whereas the metal salts had an opposite effect, namely a shift towards higher temperatures. Hence, it can be stated that the solute incorporated to the aqueous phase had the same effect on the microemulsions stabilised by pure $C_{12}E_4$ and technical grade Brij30 surfactant, respectively, and this feature was not affected by the presence of 1-octanol as co-surfactant in the latter system.

As we are finally aiming at the synthesis of bimetallic particles, the funnel diagrams of the microemulsions containing two metal salts were also determined (Figure S2 in Supporting Material). The presence of a stoichiometric mixture of H_2PtCl_6 and $Pb(NO_3)_2$ had a similar impact on the location of the phase boundaries as the addition of one of the two metal precursors, namely a weak shift towards higher temperatures. In case of a stoichiometric mixture of H_2PtCl_6 and $Bi(NO_3)_3$ there was a significant shift upwards due to the presence of 2M HNO_3 needed to solubilise 0.011 M $Bi(NO_3)_3$ in 0.011 M H_2PtCl_6 aqueous solution as stated in Section 2.2.

3.2.1 Tuning the *wefb* of H_2O/solute – *n*-octane – Brij30/1-octanol

We have shown that 1-octanol had to be added to the Brij30-based microemulsions in order to obtain the one phase region of the funnel diagram in a temperature range similar to that found for the $C_{12}E_4$-based microemulsions. This can be understood by the fact that titrating 1-octanol to the ternary system **H_2O – *n*-octane – Brij30** reduces the average head group size per molecule in the surfactant layer and thus decreases the curvature of the oil-water interface. In other words, the presence of an alcohol with a relatively long alkyl chain makes the interface more hydrophobic and thus counterbalances the effect of hydrophilic $C_{12}E_j$ surfactants ($j > 4$). Consequently, the temperature at which the *wefb* occurs decreases

continuously by titrating 1-octanol irrespective of the composition of the aqueous phase (see Figure S3 in Supporting Material illustrating the case of the microemulsion containing the reducing agent).

Despite the fact that the microemulsion becomes more complex by adding 1-octanol, one can use the co-surfactant as a tuning parameter to match the *wefb* of microemulsions containing the metal salt and the reducing agent, respectively. We emphasize again that this procedure has to be carried out since the metal salt and the reducing agent have an opposite effect on the location of the *wefb*. The overlap of the two *wefb* at constant water content w_A can be performed either by decreasing the 1-octanol content of the microemulsion containing the reducing agent or by increasing the 1-octanol concentration of the microemulsion containing the metal salt. We show in Figure 7 that an overlap can indeed by decreasing the octanol content in the $NaBH_4$-containing microemulsion. Note that the overlap of the two *wefb*s was obtained with two slightly different pairs of parameters γ_b and δ and thus the droplet sizes calculated according to ref. [18] are slightly different. For example, the diameter of the water droplets at $w_A = 0.08$ was estimated to be 14.5 ± 1.5 nm for the microemulsion containing 0.02 M H_2PtCl_6 and 16 ± 1 nm for the microemulsion containing 0.16 M $NaBH_4$. These microemulsions were thereafter used as the precursor microemulsions in synthesizing Pt and Pb nanoparticles, and the size characterization of those particles is currently under study.

4. Conclusions

The main goal of this study was a systematic investigation of the effect of various electrolytes on the phase boundaries of microemulsions stabilised by non-ionic alkyl polyethylene oxide surfactants. Platinum, lead and bismuth metal salts representing the precursors of the desired metallic particles, as well as the reducing agent $NaBH_4$ were solubilised in the aqueous phase of **H_2O – *n*-octane – $C_{12}E_4$** and **H_2O – *n*-octane – Brij30/1-octanol** microemulsions. The

strategy was to determine the funnel (one-phase) diagram of the respective systems and thus the location of the water emulsification failure boundary, *wefb*. The latter is of particular interest since it is known that the aqueous phase forms spherical droplets dispersed in the continuous oil phase at this phase boundary.

Although it was expected that the use of non-ionic surfactants minimizes the effect of electrolytes on the location of the phase boundaries, it turned out that the location of the *wefb* strongly depends on the composition of the aqueous phase. Taking as references the systems **H_2O – *n*-octane – $C_{12}E_4$** and **H_2O – *n*-octane – Brij30/1-octanol**, respectively, the metal salts shifted the phase boundary towards higher temperature, whereas the reducing agent lowered the temperature of the phase boundaries. It was argued that the location of the *wefb* is determined by the salting-in and salting-out effect of the additives presented in the aqueous phase. These effects depend in a complex manner on the ionc strength, the pH (the lower the pH the higher the temperature at which the *wefb* occurred), and on the specific ions. Although details are not understood yet it became obvious that the *wefb* shift of the H_2PtCl_6- and the $Bi(NO_3)_3$-containing microemulsions is due to the low pH, the *wefb* shift of the $NaBH_4$-containing system is due to the high pH, and the *wefb* shift of the $Pb(NO_3)_2$-containing system is due to the salting-in effect of NO_3^-.

The next step was to adjust the phase boundaries of the systems **H_2O/solute – *n*-octane – $C_{12}E_4$** such that the *wefb* of the metal salt-containing and that of the reducing agent-containing microemulsion overlap, which could be carried out by adding NaOH for the H_2PtCl_6-containing microemulsion only. The addition of NaOH to the solution of the metal salt shifted the *wefb* towards lower temperatures such that it became similar to the *wefb* of the $NaBH_4$-containing system. Unfortunately an increase of the pH and thus a decreae of the *wefb* was impossible for the $Pb(NO_3)_2$- and the $Bi(NO_3)_3$-containing microemulsions due to the formation of lead oxides and the insolubility of $Bi(NO_3)_3$.

The problem encountered for the pure $C_{12}E_4$ could be resolved by tuning the *wefb* via the addition of 1-octanol. For economic reasons a technical grade surfactant was used and overlapping *wefb* were obtained by titrating the systems with 1-octanol. We have demonstrated that one can indeed obtain water-in-oil droplet microemulsions with *same water contents* w_A but different compositions (metal salt(s) or reducing agent) at the *same* temperature. The resulting phase diagrams are the basis for controlled synthesis of Pt, Bi, Pb, Pt:Pb and Pt:Bi nanoparticles via the microemulsion route using the technical grade non-ionic surfactant Brij30. Characterisation of these particles and understanding of the relationship between the size of the water droplet in the precursor microemulsion and the size of the synthesized particles is under progress.

From an application point of view it is important to note that adding multivalent metal salts or $NaBH_4$ to a microemulsion stabilised with non-ionic surfactants mainly affects the transition temperatures $\underline{2}\rightarrow 1\rightarrow \bar{2}$, while the water solubilising capacity is not changed significantly at the electrolyte concentrations investigated in the present study. This is in contrast to microemulsions stabilised by ionic surfactants where adding an electrolyte reduces the water solubilising capacity.[18]

Acknowledgment

M.M. like to thank the Science Foundation Ireland (SFI) and D.A. the UCD Center for Synthesis and Chemical Biology (CSCB) for financial support.

Table 1. Composition and phase transition temperatures T_{min} and T_{max} of **H_2O/solute – *n*-octane – $C_{12}E_4$** microemulsions at w_A = 0.06. T_{min} is the phase transition temperature between the $\underline{2}$- and the 1-phase region and T_{max} is the phase transition temperature between the 1- and the $\bar{2}$ -phase region (*wefb*). *I* and *pH* stand for the ionic strength and pH, respectively. According to eq. 5, the droplet size at w_A = 0.06 is roughly 18 ± 1 nm.

solute (w_A = 0.06)	c_{solute} / M	*I* / M	*pH*	T_{max} (*wefb*) / ºC	T_{min} / ºC
H_2O	-	-	~6	21.6	9.0
H_2PtCl_6	0.04	0.48	~1	23.4	12.0
$Pb(NO_3)_2$	0.04	0.12	~6	23.1	< 6
$Bi(NO_3)_3$ / HNO_3	0.04 / 0.32	0.56	~1	26.5	13.0
$NaBH_4$ / NaOH	0.16 / 0.16	0.32	~13	13.1	< 6
$NaBH_4$	0.16	0.16	~10	19.0	8.0
NaCl	0.16	0.16	~6	16.2	19.7
NaOH	0.16	0.16	~13	15.3	18.2
HCl	0.16	0.16	~1	17.6	21.9

References

[1] G. Siné, D. Smida, M. Limat, G. Fóti, C. Comninellis, J. Elec. Soc. 154 (2007) B170.

[2] J. Solla-Gullón, F.J. Vidal-Iglesias, V. Montiel, A. Aldaz, Electrochim. Acta 49 (2004) 5079.

[3] S. Rojas, F.J. Garcia-Gracia, S. Jaras, M.V. Martinez-Huerta, J.L. Garcia-Fierro, M. Boutonnet, Appl. Catal., A 285 (2005) 24.

[4] M. Boutonnet, J. Kizling, R. Touroude, G. Marie, P. Stenius, Catal. Lett. 9 (1991) 347.

[5] J. Fang, K.L. Stokes, J.A. Wiemann, W.L. Zhou, J. Dai, F. Chen, C.J. O'Connor, Mater. Sci. Eng. B83 (2001) 254.

[6] K. Naoe, C. Petit, M.P. Pileni, Langmuir 24 (2008) 2792.

[7] M.-P. Pileni, Nature Materials 2 (2003) 145.

[8] H.H. Ingelsten, R. Bagwe, A. Palmqvist, M. Skoglundh, C. Svanberg, K. Holmberg, D.O. Shah, J. Coll. Int. Sci. 241 (2001) 104.

[9] M.-L. Wu, D.-H. Chen, T.-C. Huang, Langmuir 17 (2001) 3877.

[10] P. Calandra, C. Giordano, A. Longob, V.T. Liveri, Mater. Chem. Phys. 98 (2006) 494.

[11] I. Capek, Adv. Coll. Int. Sci. 110 (2004) 49.

[12] K. Holmberg, J. Coll. Int. Sci. 274 (2004) 355.

[13] M. Boutonnet, S. Lögdberg, E.E. Svensson, Curr. Opin. Col. Int. Sci. 13 (2008) 270.

[14] S. Qiu, J. Dong, G. Chen, J. Coll. Int. Sci. 216 (1999) 230.

[15] J. Lin, Y. Lin, P. Liu, M.J. Meziani, L.F. Allard, Y.-P. Sun, J. Am. Chem. Soc. 124 (2002) 11514.

[16] D.R.M. Godoi, J. Perez, H.M. Villullas, J. Electrochem. Soc. 154 (2007) B474.

[17] D.H. Chen, C.J. Chen, J. Mater. Chem. 12 (2002) 1557.

[18] C. Stubenrauch, T. Wielpütz, T. Sottmann, C. Roychowdhury, F.J. DiSalvo, Coll. and Surf. A: Physicochem. Eng. Aspects 317 (2008) 328.

[19] M. Watanabe, K. Tsurumi, T. Mizukami, T. Nakamura, P. Stonehart, J. Electrochem. Soc. 141 (1994) 2659.

[20] K. Yohannes, J. Electrochem. Soc. 143 (1996) 2152.

[21] A. Lewera, W.P. Zhoua, C. Vericat, J.H. Chunga, R. Haasch, A. Wieckowski, P.S. Bagus, Electrochim. Acta 51 (2006) 3950.

[22] E. Casado-Rivera, Z. Gal, A.C.D. Angelo, C. Lind, F.J. DiSalvo, H.D. Abruňa, Chem. Phys. Chem. 4 (2003) 193.

[23] E. Casado-Rivera, D.J. Volpe, L. Alden, C. Lind, C. Downie, T. Vazquez-Alvarez, A.C.D. Angelo, F.J. DiSalvo, H.D. Abruňa, J. Am. Chem. Soc. 126 (2004) 4043.

[24] H. Wang, L. Alden, F.J. DiSalvo, H.D. Abruňa, Phys. Chem. Chem. Phys. 10 (2008) 3739.

[25] H.D. Abruňa, F. Matsumoto, J.L. Cohen, J. Jin, C. Roychowdhury, M. Prochaska, R.B.van Dover, F.J. DiSalvo, Y. Kiya, J.C. Henderson, G.R. Hutchison, Bull. Chem. Soc. Jpn. 80 (2007) 1843.

[26] D. Xia, G. Chen, Z. Wang, J. Zhang, S.R. Hui, D. Ghosh, H. Wang, Chem. Mater. 18 (2006) 5746.

[27] L.R. Alden, C. Roychowdhury, F. Matsumoto, D.K. Han, V.B. Zeldovich, H.D. Abruňa, F.J. DiSalvo, Langmuir 22 (2006) 10465.

[28] C. Roychowdhury, F. Matsumoto, V.B. Zeldovich, S.C. Warren, P.F. Mutolo, M.J. Ballesteros, U. Wiesner, H.D. Abruňa, F.J. DiSalvo, Chem. Mater. 18 (2006) 3365.

[29] F. Matsumoto, C. Roychowdhury, F.J. DiSalvo, H.D. Abruňa, J. Electrochem. Soc. 155 (2008) B148.

[30] M. Jitianu, R. Kleisinger, M. Lopez, D.V. Goia, J. New Mater. Electrochem. Sys. 10 (2007) 67.

[31] M.J. Escudero, E. Hontanon, S. Schwartz, M. Boutonnet, L. Daza, J. Power Sources 106 (2002) 206.

[32] X. Zhang, K.-Y. Chan, J. Mater. Chem. 12 (2002) 1203.

[33] A.R. Malheiro, L.C. Varanda, J. Perez, H.M. Villullas, Langmuir 23 (2007) 11015.

[34] L.G.R.A. Santos, C.H.F. Oliveira, I.R. Moraes, E.A. Ticianelli, J. Electroanal. Chem. 596 (2006) 141.

[35] L. Xiong, A. Manthiram, Electrochim. Acta 50 (2005) 2323.

[36] M.L. Wu, K.B. Lai, Coll. Surf. A 244 (2004) 149.

[37] M.L. Wu, D.H. Chen, T.C. Huang, Chem. Mater. 13 (2001) 599.

[38] M. Yashima, L.K.L. Falk, A.E.C. Palmqvist, K. Holmberg, J. Coll. Int. Sci. 268 (2003) 348.

[39] M.L. Wu, D.H. Chen, T.C. Huang, J. Coll. Int. Sci 243 (2001) 102.

[40] A. Bumajdad, J. Eastoe, M.I. Zaki, R.K. Heenan, L. Pasupulety, J. Coll. Int. Sci 312 (2007) 68.

[41] R. Najjar, C. Stubenrauch, J. Coll. Int. Sci 331 (2009) 214.

[42] R. Strey, Coll. Polym. Sci. 272 (1994) 1005

[43] L. Belkoura, C. Stubenrauch, R. Strey, Langmuir 20 (2004) 4391.

[44] T. Sottmann, R. Strey, in: Fundamentals of Interface and Colloid Science, J. Lyklema, (Ed.) Elsevier: Amsterdam, 2005; Vol. V Soft Colloids, Chapter 5.

[45] M.d. Dios, F. Barroso, C. Tojo, M.A. López-Quintela, J. Coll. Int. Sci. (2009) in press.

[46] J. Solla-Gullon, A. Rodes, V. Montiel, A. Aldaz, J. Clavilier, J. Electroanal. Chem. 554-555 (2003) 273.

[47] A. Evilevitch, U. Olsson, B. Jönsson, H. Wennerström, Langmuir 16 (2000) 8755.

[48] Y. Luo, X. Sun, Mater. Lett. 61 (2007) 2015.

[49] C.-L. Lee, C.-C. Wan, Y.-Y. Wang, Adv. Funct. Mat. 11 (2001) 344.

[50] T. Sottmann, R. Strey, in: Soft Colloids V, J. Lyklema, (Ed.) Elsevier: Amsterdam, 2005.

[51] T. Sottmann, Bunsen Mag. 6 (2006) 163.

[52] K. Kon-on, A. Kitahara, J. Coll. Int. Sci 41 (1972) 47.

[53] M. Kahlweit, R. Lessner, R. Strey, J. Phys. Chem. 87 (1983) 5032.

[54] K. Shinoda, H. Takeda, J. Coll. Int. Sci 32 (1970) 642.

[55] H. Schott, J. Coll. Int. Sci 43 (1973) 150.

[56] A. Shaheen, N. Kaur, R.K. Mahajan, Colloid Polym. Sci. 286 (2008) 319.

[57] H. Schott, A.E. Royce, S.K. Han, J. Coll. Int. Sci 96 (1984) 196.

[58] Y. Zhang, P.S. Cremer, Curr. Op. Chem. Biol. 10 (2006) 658.

[59] Note that our results are not in line with the results pulished by Tourode et al. (R. Touroude; P. Bernardt; G. Maire; J. Kizling; M. Boutonnet; P. Stenius, in: Organized Solutions, S. E. Friberg; B. Lindman, (Eds.) Marcel Dekker Inc.: New York, 1992) who found that adding H_2PtCl_6 to the system H_2O – n-dodecane – $C_{12}E_5$ shifts the phase boundaries towards lower temperatures. We remeasured the effect of the platinum salt on the phase boundaries of this system and found a shift towards higher temperatures in agreement with our observations for H_2O – n-octane – $C_{12}E_4$. Thus we believe that the observation made by Tourode et al. is either an experimental error or due to the fact that they used a commercial product which they purified via distillation.

Figure Captions

Figure 1. $T(w_A)$-sections through the phase diagram of the ternary base system H_2O – *n*-octane – $C_{12}E_4$ (black circles) and the system H_2O/metal salt – *n*-octane – $C_{12}E_4$ (white symbols) at $\gamma_b = 0.06$ with (a) 0.04 M H_2PtCl_6 (white circles), (b) 0.04 M $Pb(NO_3)_2$ (white triangles), and (c) 0.04 M $Bi(NO_3)_3$ + 0.32 M HNO_3 (white diamonds). (1) stands for the one-phase microemulsion region, ($\underline{2}$) for an oil-in-water microemulsion coexisting with an oil phase, and ($\overline{2}$) for a water-in-oil microemulsion coexisting with an excess water phase.

Figure 2. $T(w_A)$-sections through the phase diagram of the system H_2O/$NaBH_4$ – *n*-octane – $C_{12}E_4$ at $\gamma_b = 0.06$ with 0 M $NaBH_4$ (black circles), 0.16 M $NaBH_4$ (gray circles), and 0.16 M $NaBH_4$ + 0.16 M NaOH (gray squares).

Figure 3. The water emulsification failure boundary, *wefb* ($1 \rightarrow \overline{2}$) and the $\underline{2} \rightarrow 1$ boundary of the system H_2O/solute – *n*-octane – $C_{12}E_4$ as a function of the pH at $\gamma_b = 0.06$, $w_A = 0.06$, and $I = 0.16$ M (boundaries determined by turbidity measurements). The pH was adjusted by HCl and NaOH, respectively.

Figure 4. $T(w_A)$-sections through the phase diagram of the system H_2O/solute – *n*-octane – $C_{12}E_4$ at $\gamma_b = 0.06$ with 0.04 M H_2PtCl_6 (white circles), 0.04 M H_2PtCl_6 + 0.16 M NaOH (white squares), and 0.16 M $NaBH_4$ (gray circles).

Figure 5. $T(w_A)$-sections through the phase diagram of the systems H_2O – *n*-octane – $C_{12}E_4$ at $\gamma_b = 0.06$ (black circles), H_2O – *n*-octane – Brij30 at $\gamma_b = 0.06$ (black diamonds), and H_2O

– *n*-octane – Brij30/1-octanol at γ_b = 0.114 and δ = 0.376 (black squares); the phase boundaries of the latter system were determined by turbidity measurements.

Figure 6. $T(w_A)$-sections through the phase diagram of the systems H_2O – *n*-octane – Brij30/1-octanol (black squares), $H_2O/NaBH_4$ – *n*-octane – Brij30/1-octanol with $NaBH_4$ = 0.16 M (gray circles), and H_2O/metal salt – *n*-octane – Brij30/1-octanol (white symbols) at γ_b = 0.114 and δ = 0.376. (a) H_2PtCl_6 = 0.02 M (white circles) and (b) $Pb(NO_3)_2$ = 0.04 M (white squares).

Figure 7. $T(w_A)$-sections through phase diagram of the system H_2O/solute – *n*-octane – Brij30/1-octanol. (a) 0.02 M H_2PtCl_6 at γ_b = 0.114 and δ = 0.376 (white symbols), 0.16 M $NaBH_4$ at γ_b = 0.097 and δ = 0.221 (gray symbols); (b) 0.04 M $Pb(NO_3)_2$ at γ_b = 0.114 and δ = 0.376 (white symbols), 0.16 M $NaBH_4$ at γ_b = 0.092 and δ = 0.200 (gray symbols). Note that the γ_b- and the δ-values of the $NaBH_4$-containing microemulsion were adjusted in order to have overlapping phase boundaries of both microemulsions.

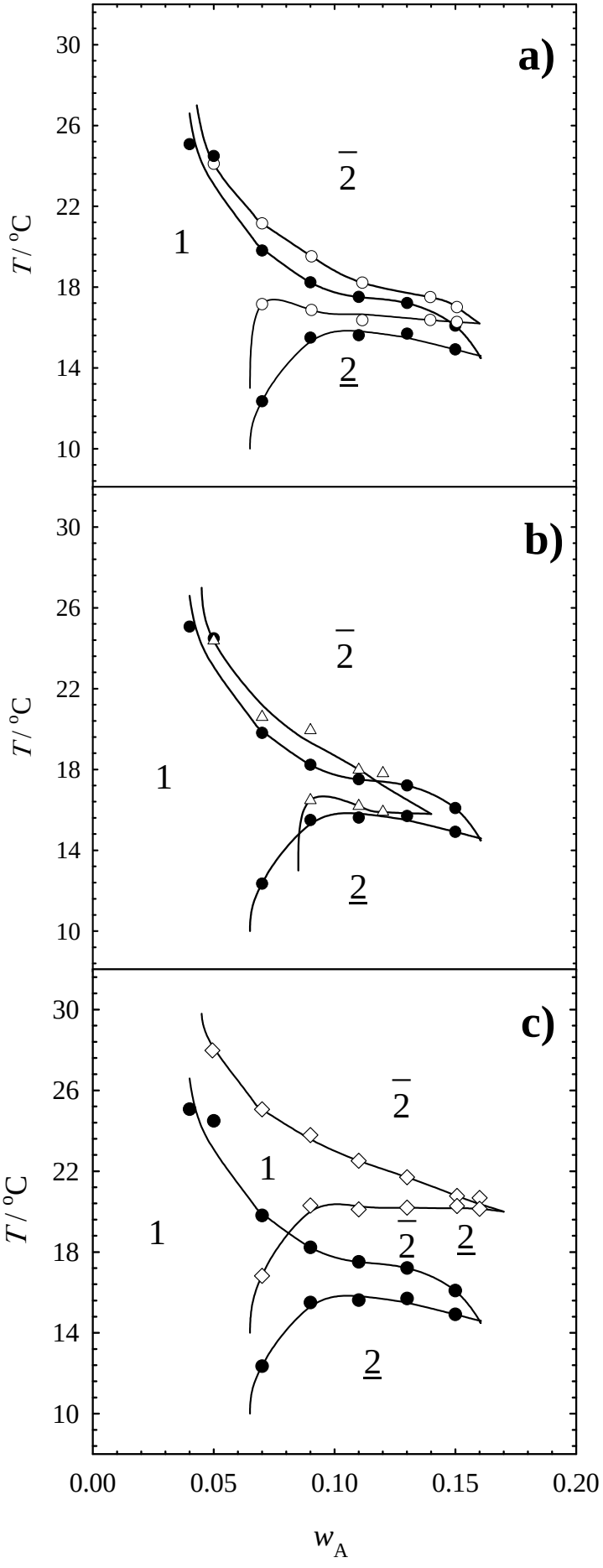

Figure 1

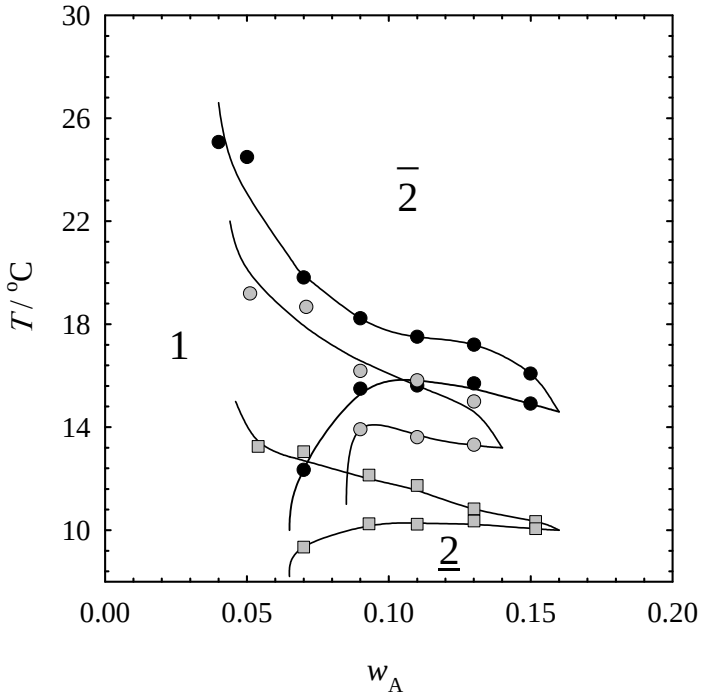

Figure 2

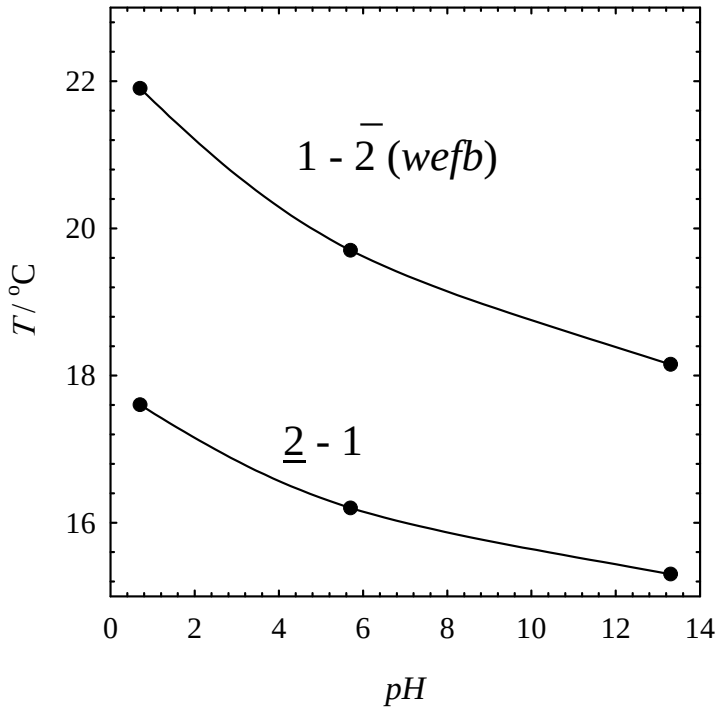

Figure 3

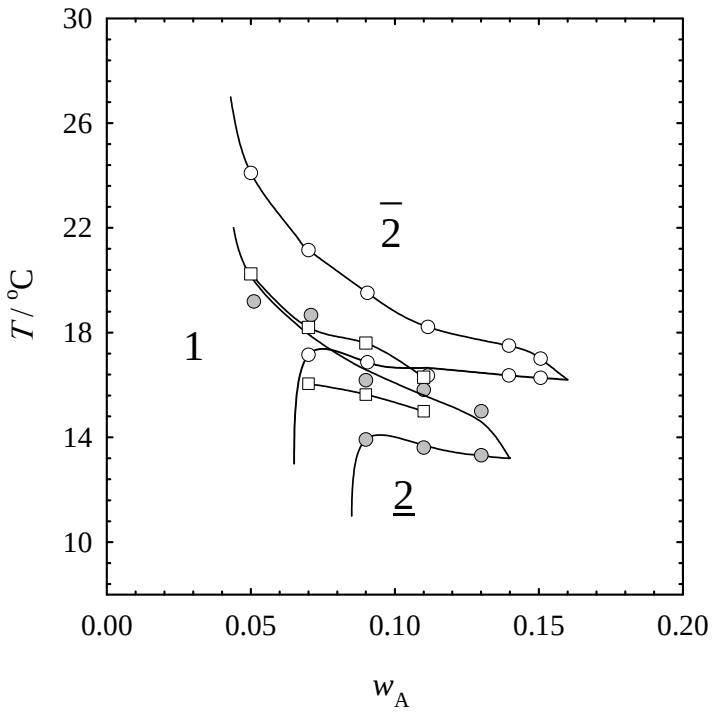

Figure 4

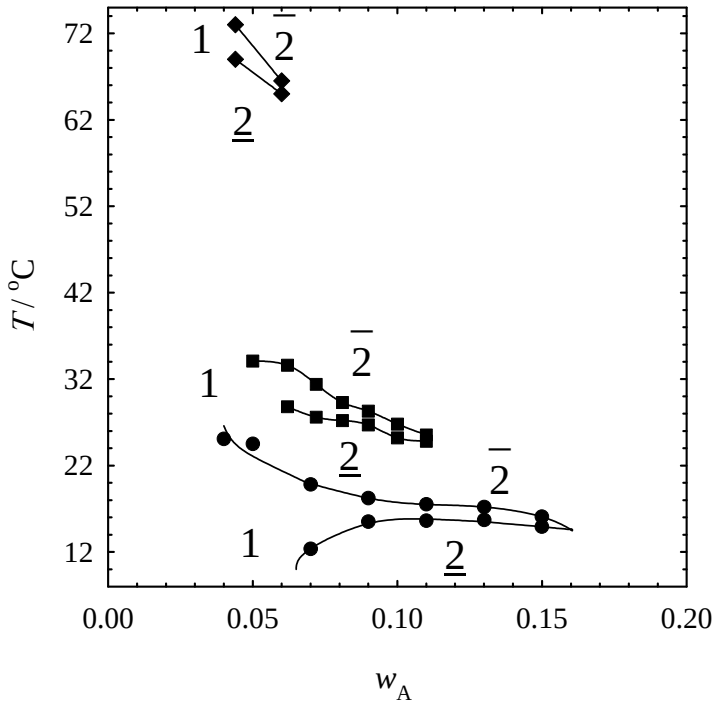

Figure 5

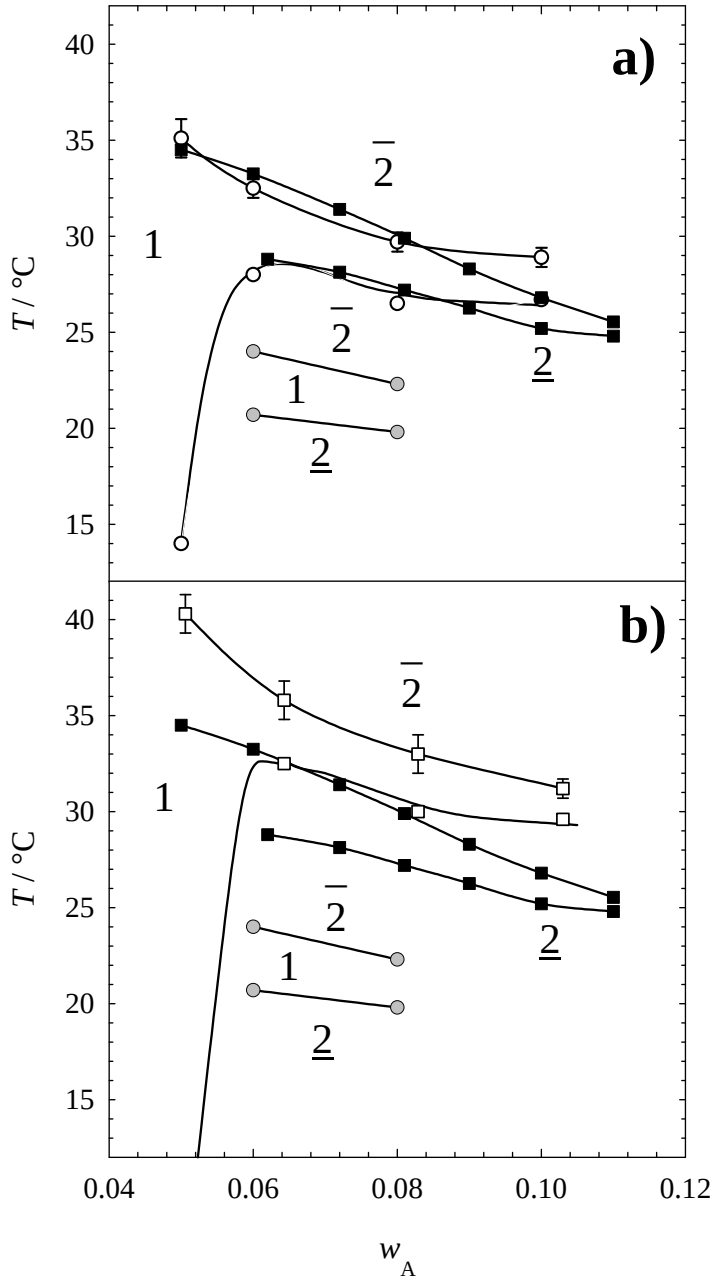

Figure 6

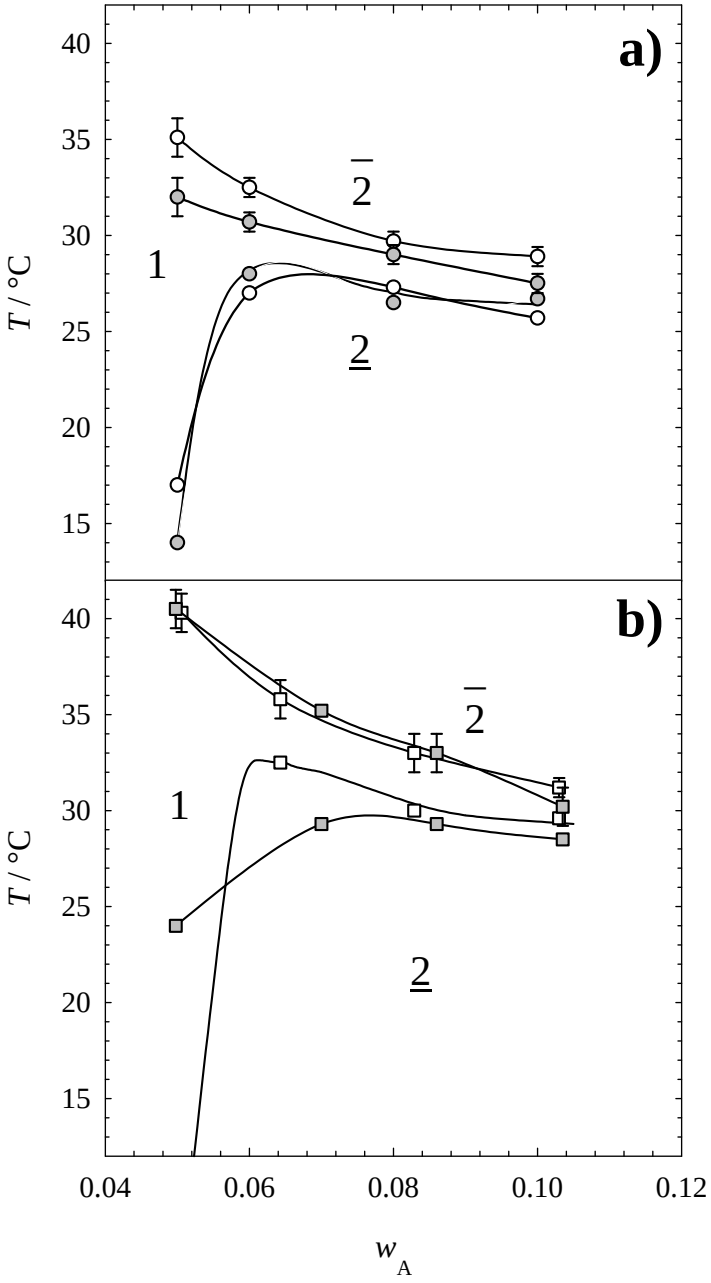

Figure 7

Supporting Materials Section

S1 Phase diagram of H_2O/NaCl – *n*-octane – $C_{12}E_4$

Comparing the location of the two phase boundaries, *i.e. wefb* and $\underline{2}\rightarrow 1$, of the salt-free and the salt-containing system (Figure S1), it was found that (i) the surfactant efficiency slightly decreases as the critical end point, i.e. the intersection of the two boundaries, is found at lower water content, (ii) the whole funnel diagram is shifted towards lower temperatures, and (iii) the two funnel diagrams extend over similar temperature ranges at $w_A < 0.1$. The second feature is due to the fact that the electrolyte competes with the surfactant for hydration water. As less hydration water is available for $C_{12}E_4$, the average curvature of the surfactant layer is lower than for the salt-free system and thus the transition $\underline{2}\rightarrow 1\rightarrow \overline{2}$ takes place at lower temperatures.

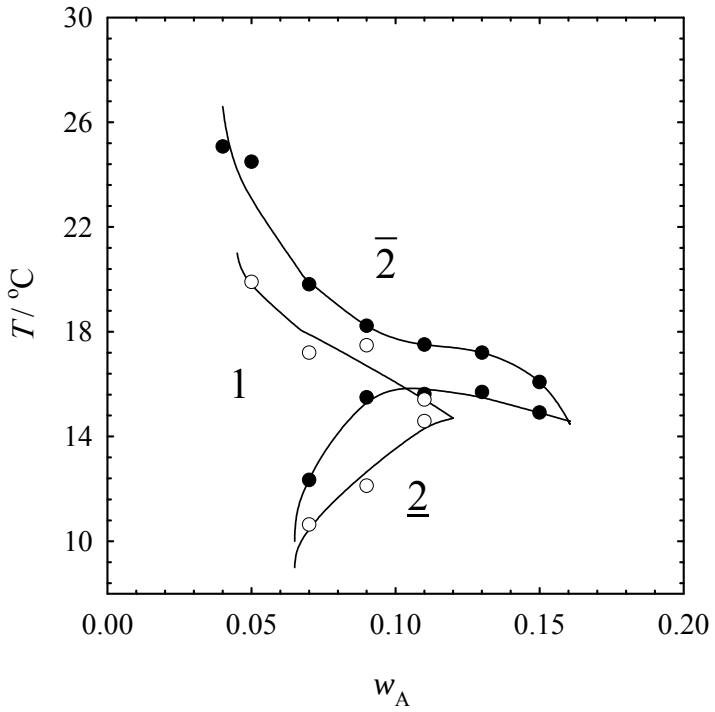

Figure S1. $T(w_A)$-sections through the phase diagram of the ternary base system H_2O – *n*-octane – $C_{12}E_4$ (black symbols) and the system H_2O/NaCl – *n*-octane – $C_{12}E_4$ (white symbols) at $\gamma_b = 0.06$; NaCl = 0.16 M.

S2 Phase diagrams of H_2O/metal salts – *n*-octane – Brij30/1-octanol

Figure S2 displays the $T(w_A)$-section of microemulsions containing two stoichiometric mixtures of metal salts, namely 0.013 M H_2PtCl_6 + 0.013 M $Pb(NO_3)_2$ and 0.011 M H_2PtCl_6 + 0.011 M $Bi(NO_3)_3$, respectively. For the sake of completeness, the funnel diagrams of the reference system and of the system containing 0.16 M $NaBH_4$ (reducing agent) are also shown at the same γ_b and δ. The presence of more than one metal salt in the aqueous phase does not have a significant impact on the location of the phase boundary (see Figure S2a and 6a) and consequently the expected mismatch of the *wefb* of the microemulsions containing two metal salt(s) and reducing agent, respectively, occurred. Note that the large shift towards higher temperatures observed for the aqueous mixture 0.011 M H_2PtCl_6 + 0.011 M $Bi(NO_3)_3$ (Figure S2b) arises from the presence of large amounts of HNO_3 which was needed to solubilise $Bi(NO_3)_3$.

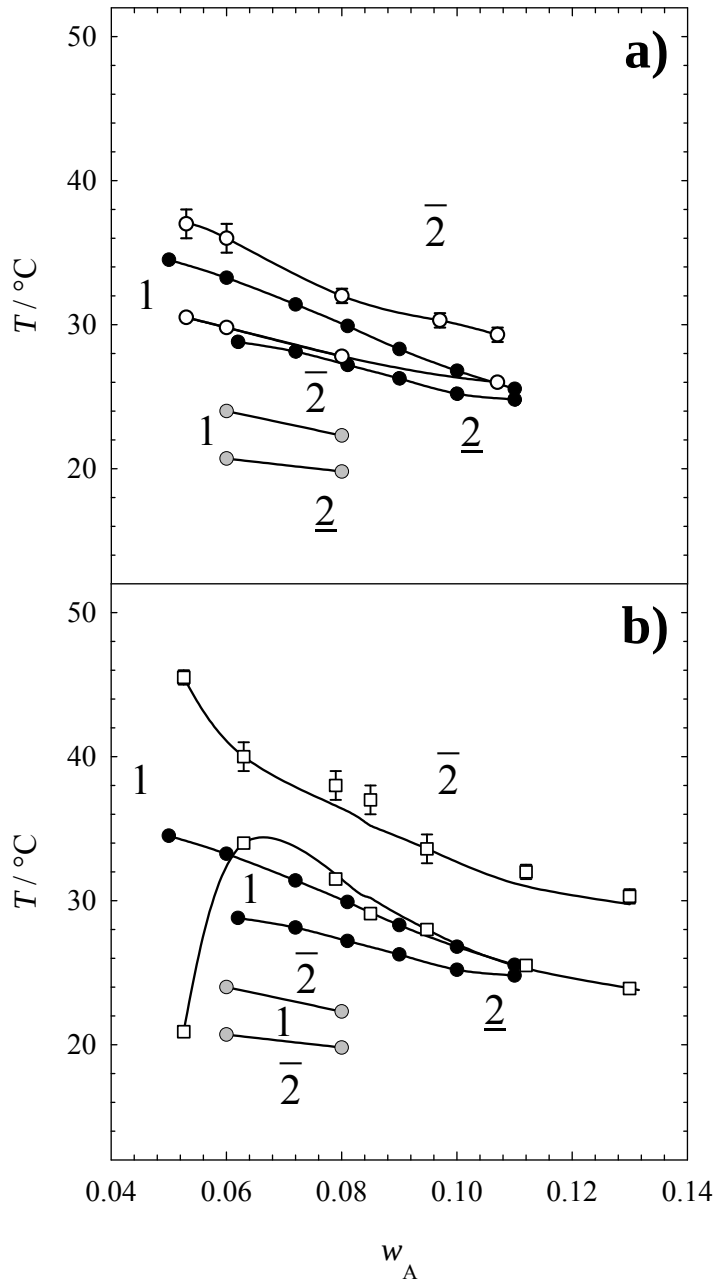

Figure S2. $T(w_A)$-section through the phase diagram of the systems H_2O (black symbols) / metal salt (white symbols) / reducing agent (gray symbols) – *n*-octane – Brij30/1-octanol at $\gamma_b = 0.114$ and $\delta = 0.376$; $NaBH_4 = 0.16$ M, (a) $H_2PtCl_6 = 0.013$ M and $Pb(NO_3)_2 = 0.013$ M and (b) $H_2PtCl_6 = 0.011$ M, $Bi(NO_3)_3 = 0.011$ M and $HNO_3 = 2$ M.

S3 Titration of the system $H_2O/NaBH_4$ – *n*-octane – Brij30 with 1-octanol

As was shown in Figure 5, adding 1-octanol decreased significantly the temperature where the one-phase region is found in the phase diagram, and we claimed that 1-octanol is a tuning parameter for the *wefb*. Additional support of this statement is given by Figure S3 where the temperature of the *wefb* is plotted at constant $w_A = 0.08$ as a function of γ_b for the systems **H_2O – *n*-octane – Brij30/1-octanol** and **$H_2O/NaBH_4$ – *n*-octane – Brij30/1-octanol, respectively.** It is seen that the *wefb* shifts towards lower temperatures with increasing γ_b and finally seems to level off at large γ_b. The data were obtained by titrating 1-octanol to the systems. The difference between the $NaBH_4$-free and the $NaBH_4$-containing system is mainly due to the salting out effect of $NaBH_4$.

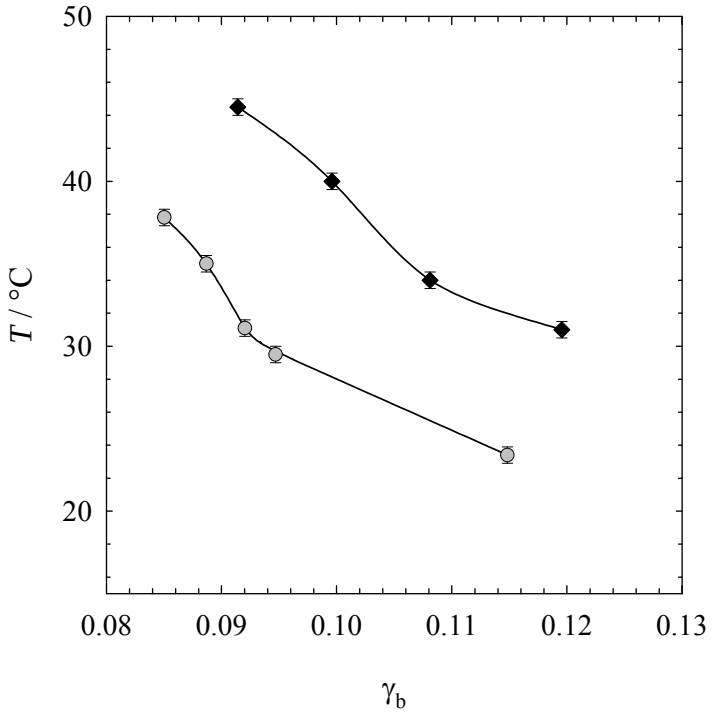

Figure S3. The *wefb* of the systems $H_2O/NaBH_4$ – *n*-octane – Brij30/1-octanol as a function of γ_b at $w_A = 0.08$ with 0 M $NaBH_4$ (black diamonds) and 0.16 M $NaBH_4$ (gray circles). Note that γ_b was varied by titrating 1-octanol to the system, i.e. δ changes with increasing γ_b (for the alcohol-free system it holds $\delta = 0$, $\gamma_b = 0.075$).